PHYSICAL REVIEW B **89**, 045112 (2014)

Pressure-induced valence change of $YbNiGe_3$ investigated by resonant x-ray emission spectroscopy at the Yb L_3 edge

Hitoshi Sato,[1,*] Hitoshi Yamaoka,[2] Yuki Utsumi,[3,†] Heisuke Nagata,[3] Marcos A. Avila,[4] Raquel A. Ribeiro,[4] Kazunori Umeo,[5] Toshiro Takabatake,[6,7] Yumiko Zekko,[8] Jun'ichiro Mizuki,[8,9] Jung-Fu Lin,[10] Nozomu Hiraoka,[11] Hirofumi Ishii,[11] Ku-Ding Tsuei,[11] Hirofumi Namatame,[1] and Masaki Taniguchi[1,3]

[1]*Hiroshima Synchrotron Radiation Center, Hiroshima University, Kagamiyama 2-313, Higashi-Hiroshima 739-8526, Japan*
[2]*RIKEN SPring-8 Center, Sayo, Hyogo 679-5148, Japan*
[3]*Graduate School of Science, Hiroshima University, Kagamiyama 1-3-1, Higashi-Hiroshima 739-8526, Japan*
[4]*Centro de Ciências Naturais e Humanas, Universidade Federal do ABC, Santo Andrê - SP, 09210-971, Brazil*
[5]*Cryogenics and Instrumental Analysis Division, N-BARD, Hiroshima University, Higashi-Hiroshima 739-8526, Japan*
[6]*Department of Quantum Matter, AdSM, Hiroshima University, Higashi-Hiroshima 739-8530, Japan*
[7]*Institute for Advanced Materials Research, Hiroshima University, Higashi-Hiroshima 739-8530, Japan*
[8]*Graduate School of Science and Technology, Kwansei Gakuin University, Sanda, Hyogo 669-1337, Japan*
[9]*Japan Atomic Energy Agency, SPring-8, Sayo, Hyogo 679-5148, Japan*
[10]*Department of Geological Sciences, The University of Texas at Austin, Austin, Texas 78712, USA*
[11]*National Synchrotron Radiation Research Center, Hsinchu 30076, Taiwan*

(Received 26 November 2013; revised manuscript received 29 December 2013; published 10 January 2014)

Pressure dependence of the Yb valence in $YbNiGe_3$ has been investigated up to 15.6 GPa at 300 K and up to 7.7 GPa at 17 K by means of x-ray absorption spectroscopy in $L\alpha_1$ partial fluorescence yield mode and resonant x-ray emission spectroscopy around the Yb L_3 absorption edge. The Yb valence in $YbNiGe_3$ at ambient pressure strongly fluctuates with the mean valence of $v = 2.52 \pm 0.01$ at 300 K. The Yb valence rapidly changes toward a trivalent state with pressure up to ~5 GPa, slowly increases up to ~10 GPa, and then reaches a saturated value of $v \sim 2.87$ at 15.6 GPa. The Yb valence at 17 K slightly decreases compared to that at 300 K; $v \sim 2.45$ at ambient pressure and ~2.72 at 7.7 GPa. We found that the pressure-induced change in the intensity of a quadrupole component in the x-ray absorption spectra shows the same trend as the Yb valence in $YbNiGe_3$. In contrast to $YbNiGe_3$, the Yb valence in $YbNiSi_3$ is nearly 3 at ambient pressure with almost no temperature dependence.

DOI: 10.1103/PhysRevB.89.045112 PACS number(s): 74.62.Fj, 75.30.Mb, 78.70.Ck, 78.70.En

I. INTRODUCTION

Kondo-lattice systems such as Ce and Yb-based heavy-fermion compounds have attracted a great deal of attention thus far. The competition between the intersite Ruderman-Kittel-Kasuya-Yosida (RKKY) interaction and the on-site Kondo effect is the key concept of these systems. When the RKKY interaction is dominant, the Ce or Yb $4f$ moments are stabilized and order magnetically at low temperature. When the Kondo effect is dominant, on the other hand, the $4f$ moments are screened by conduction electrons and the systems exhibit Fermi liquid behavior without magnetic ordering at low temperature. The competition between the two interactions can be summarized in the Doniach phase diagram [1]. The point separating the magnetic and nonmagnetic regions at 0 K in the phase diagram, where the ground state changes from a magnetically ordered state to a nonmagnetic state, is the so-called quantum critical point (QCP).

In the study of $4f$ electron systems, one of the most important issues is to establish the electronic structure in the vicinity of the QCP. Quantum fluctuations can produce unconventional physical properties such as a non-Fermi liquid state and a heavy-fermion superconductivity. Unconventional superconductivity is found in many Ce-based heavy fermion compounds, which is considered to be mediated by magnetic fluctuations around the QCP [2–4]. On the other hand, far fewer studies have been done for the Yb compounds, partly because of the difficulty of sample preparation. Within the Yb-based compounds, the first heavy-fermion superconductor β-$YbAlB_4$ with $T_c = 80$ mK was discovered a few years ago [5], whose position in the Doniach diagram is located very close to the QCP. Its Yb valence is revealed to strongly fluctuate with a mean value of $v \sim 2.75$ using hard x-ray photoemission spectroscopy [6]. It has been pointed out that valence fluctuation plays an important role for the quantum criticality and superconductivity in β-$YbAlB_4$ [7].

The balance between the RKKY and Kondo effect in the $4f$ electron systems and consequently their positions in the Doniach diagram can be controlled by pressure through the change of an exchange interaction between the $4f$ and conduction electrons. In case of the Yb compounds, a transition from the nonmagnetic to magnetically ordered states possibly takes place through the QCP at a critical pressure (P_c). Transport measurements under pressure have become more actively carried out recently in order to search for the pressure-induced QCPs for the Yb compounds. Understanding the relation between the transport properties and the Yb valence under pressure is highly relevant in these studies. Recently Fernandez-Pañella *et al*. investigated the Yb valence in $YbCu_2Si_2$ with a pressure-induced ferromagnetic order at $P_c \sim 8$ GPa [8] by means of x-ray absorption spectroscopy in the Yb $L\alpha_1$ partial fluorescence yield mode (PFY-XAS) and resonant x-ray emission spectroscopy (RXES) around the

*jinjin@hiroshima-u.ac.jp
†Present address: Max Planck Institute for Chemical Physics of Solids, Nöthnizer Straβe 40, 01187 Dresden, Germany.

Yb L_3 absorption edge under pressures up to 22 GPa [9]. In general, the Yb valence shifts toward Yb^{3+} with pressure. The authors found that the slope of the valence-pressure curve $v(P)$ becomes more gradual at 9–11 GPa, comparable to P_c. A similar change in the $v(P)$ curve near P_c was also reported for $YbNi_2Ge_2$ [10] and YbCuAl [11]. These experimental results suggest that the slope change is closely related to the QCP. The Yb valences in these compounds at 300 K are $v \sim 2.84$ for $YbCu_2Si_2$ [9], $v \sim 2.93$ for $YbNi_2Ge_2$ [10], and $v \sim 2.93$ for YbCuAl [11] at ambient pressure, and shift to $v \sim 3$ at high pressures for these compounds. Note that in these cases the Yb valence starts out already close to 3 at ambient pressure.

Here we focus on a valence fluctuating compound $YbNiGe_3$, which is located in the nonmagnetic region in the Doniach phase diagram at ambient pressure. The magnetic susceptibility shows a broad maximum at ~300 K [12], suggesting that the Kondo temperature (T_K) is substantially high and the Yb valence strongly fluctuates in comparison with $YbCu_2Si_2$, $YbNi_2Ge_2$, and YbCuAl. On the other hand, $YbNiSi_3$, where an isovalent Si is substituted for Ge in $YbNiGe_3$, exhibits an antiferromagnetic Kondo-lattice behavior with Néel temperature of $T_N = 5.1$ K, one of the highest ordering temperatures for Yb-based magnetic compounds, and its Yb valence is estimated to be $v \sim 3$ from the effective moment of $\mu_{eff} = 4.45\ \mu_B$/Yb derived form the Curie-Weiss type magnetic susceptibility above 150 K [13]. Since the lattice parameters of $YbNiSi_3$ are about 3% smaller than those of $YbNiGe_3$, the electronic state of $YbNiGe_3$ is expected to get close to that of $YbNiSi_3$ with applying pressure due to lattice contraction. Furthermore, the measurements of the temperature-dependent electrical resistivity suggest the existence of the pressure-induced QCP at approximately 8 GPa, whereby the A coefficient and residual resistivity ρ_0, defined in the form of $\rho(T) = \rho_0 + AT^n$ in the low-temperature region, steeply increase [14]. The exponent n converges to 1.6, which is close to 1.5 expected at the QCP by spin-fluctuation theory for a three-dimensional antiferromagnet [15]. Since a large change in the Yb valence is expected with pressure beyond ~8 GPa, $YbNiGe_3$ is an ideal system to examine the slope change of $v(P)$ around QCP.

In this study we have investigated the Yb valence in $YbNiGe_3$ by means of PFY-XAS and RXES around the Yb L_3 absorption edge under pressures up to 15.6 GPa at 300 K and up to 7.7 GPa at 17 K. Both the Yb^{2+} ($4f^{14}$) and Yb^{3+} ($4f^{13}$) originated structures were comparably observed in PFY-XAS and RXES spectra at ambient pressure, indicating that the Yb valence in $YbNiGe_3$ strongly fluctuates as expected. We found a pronounced change in the slope of the $v(P)$ curve between 5 and 10 GPa, across the pressure where the existence of the QCP was suggested [14], as in $YbCu_2Si_2$ [9], $YbNi_2Ge_2$ [10], and YbCuAl [11]. We also measured temperature-dependent PFY-XAS and RXES spectra of $YbNiGe_3$ at ambient pressure in comparison with $YbNiSi_3$. The Yb valence in $YbNiSi_3$ is found to be close to 3 with almost no temperature dependence, in agreement with magnetic susceptibility measurements [13].

II. EXPERIMENTS

Single crystals of $YbNiGe_3$ and $YbNiSi_3$ were grown by the Sn flux method as described in Ref. [13]. The samples were characterized by x-ray powder diffraction and electron-probe microanalysis. It is noted that $YbNiGe_3$ crystallizes into a tetragonal structure with a space group of $I4_1/amd$, while $YbNiSi_3$ assumes an orthorhombic one, $Cmmm$ [13]. Although their space groups are different, both compounds have a layered structure with a single crystallographic site for Yb and their crystal structures differ only in terms of the manner of stacking. Their crystal structure thus would be regarded as approximately the same in the present spectroscopic studies.

The PFY-XAS and RXES measurements around the Yb L_3 absorption edge were performed at the Taiwan beamline BL12XU of SPring-8 [10,16–18]. The undulator beam is monochromatized using a Si111 double crystal monochromator and focused onto the sample using troidal and K-B mirrors. A Johann-type spectrometer equipped with a spherically bent Si620 crystal (radius of ~1 m) was used to detect the Yb $L\alpha_1$ and Raman emissions with a solid state detector (XFlash 1001 type 1201). In order to reduce lifetime broadening effects and sharpen the spectral features [19], the PFY-XAS spectra were collected by monitoring the emission intensities at the emitted photon energy of $h\nu_{out} = 7416$ eV, which is the peak energy of the Yb $L\alpha_1$ fluorescence line. The overall energy resolution was estimated to be about 1 eV at $h\nu_{out} \sim 7.4$ keV. The intensities of all spectra are normalized to the incident beam intensity monitored by an ion chamber mounted just in front of the sample position. The sample temperature was cooled by a closed-circuit He cryostat down to 17 K. We used a membrane-controlled diamond anvil cell to apply pressure to the samples and silicone oil as a pressure medium. A Be gasket with 3 mm diameter and pre-indented to approximately 50 μm thick was used. The diameter of the sample chamber in the gasket was approximately 200 μm and the diamond anvil culet size was 450 μm. Pressure applied to the samples was monitored by measuring the wavelength of the R_1 fluorescence line from ruby using empirical formulas [20–22].

III. RESULTS

A. Incident energy dependence

We have measured the incident photon energy ($h\nu_{in}$) dependence of the Yb $L\alpha_1$ RXES spectra of $YbNiGe_3$ at 17 K and at ambient pressure. Figure 1(a) shows the PFY-XAS spectrum around the Yb L_3 absorption edge. Two prominent peaks at $h\nu_{in} = 8938$ and 8945 eV originate from the Yb^{2+} and Yb^{3+} $2p_{3/2} \rightarrow 5d$ transitions, respectively. Recalling that there is only one crystallographic site for Yb, this result indicates that $YbNiGe_3$ is a valence fluctuating compound as inferred from the temperature dependence of the magnetic susceptibility [12]. A weak shoulder observed at the lower $h\nu_{in}$ side of the Yb^{2+} peak ($h\nu_{in} = 8934$ eV) is ascribed to the quadrupole (QP) transition from the Yb $2p_{3/2}$ core into the empty Yb^{3+} $4f$ states, based on the comparison of the spectrum of $YbCu_2Si_2$ [23]. This shoulder is the most distinctly observed in the PFY-XAS spectrum measured at 300 K and at 15.6 GPa [Fig. 2(b)]. The QP structure is also observed for $YbNiSi_3$ as a small but clear peak at $h\nu_{in} = 8934$ eV [Fig. 4(c)]. Broad peaks around $h\nu_{in} = 8955$ and 8965 eV are a part of the oscillations due to an extended x-ray absorption fine structure (EXAFS).

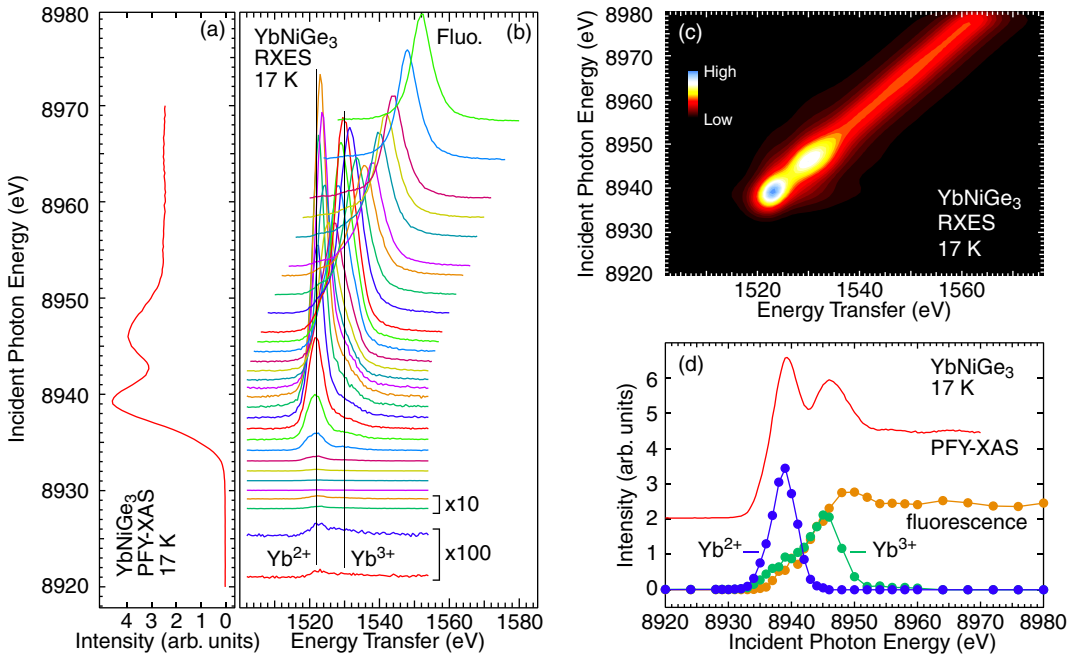

FIG. 1. (Color online) (a) PFY-XAS spectrum around the Yb L_3 absorption edge of $YbNiGe_3$ measured at 17 K and at ambient pressure. (b) Incident photon energy dependence of RXES spectra of $YbNiGe_3$ measured at 17 K and at ambient pressure. The spectra taken at $h\nu_{in} = 8920$ and 8924 eV are vertically expanded by 100 times and at $h\nu_{in} = 8928$ and 8929 eV by 10 times. Vertical offset of each spectra is scaled to $h\nu_{in}$ axis in the PFY-XAS spectrum in (a). (c) Two-dimensional image plot of (b). (d) Intensities of the Yb^{2+}- and Yb^{3+}-derived Raman components and fluorescence component as a function of $h\nu_{in}$, obtained from fits to the RXES spectra in (b).

Figure 1(b) illustrates a series of Yb $L\alpha_1$ RXES spectra of $YbNiGe_3$ measured with changing $h\nu_{in}$ from 8920 to 8968 eV, across the Yb L_3 absorption edge. The spectra are plotted as a function of energy transfer ($\Delta h\nu$), defined as difference energy between incident and emitted photon energies; $\Delta h\nu \equiv h\nu_{in} - h\nu_{out}$. The vertical offset of each

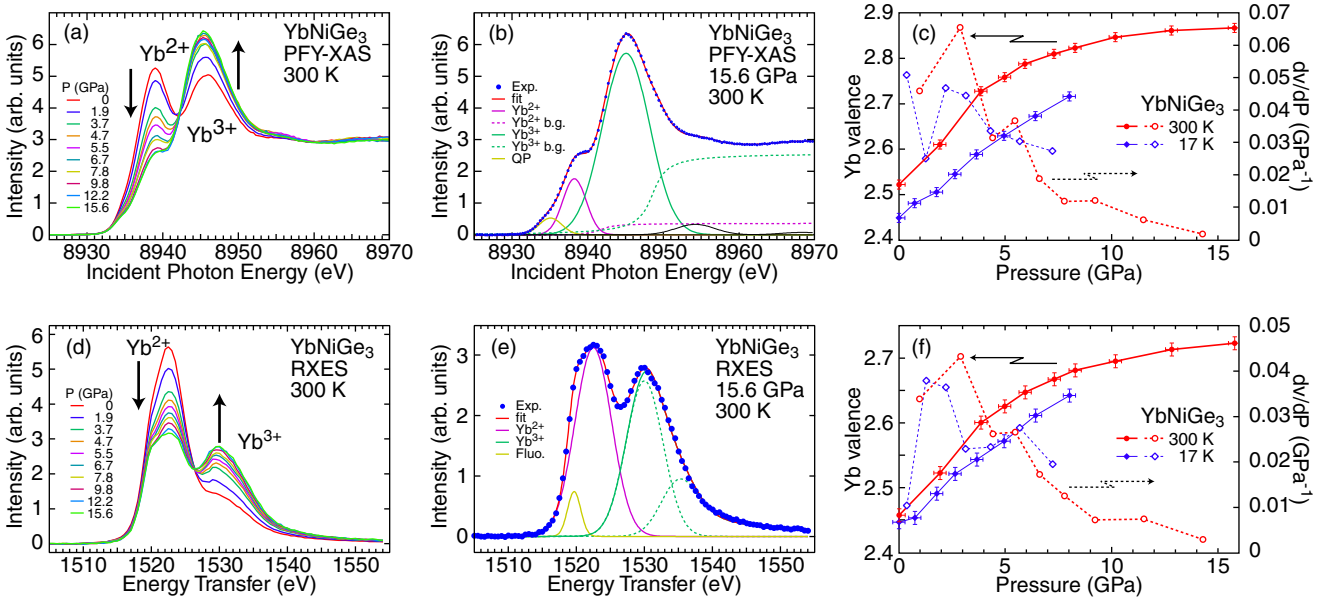

FIG. 2. (Color online) (a) Pressure dependence of Yb L_3-edge PFY-XAS spectra around the Yb L_3 absorption edge of $YbNiGe_3$ measured at 300 K. (b) Fit to PFY-XAS spectrum measured at 15.6 GPa. (c) Yb valences at 300 and 17 K as a function of pressure (solid lines with closed circles and diamonds, respectively) and the rate of change with pressure (dashed lines with open circles and diamonds, respectively) derived from the fits to the PFY-XAS spectra. (d) Pressure dependence of RXES spectra of $YbNiGe_3$ at 300 K excited with $h\nu_{in} = 8934$ eV. (e) Fit to RXES spectrum measured at 15.6 GPa. (f) Yb valences at 300 and 17 K as a function of pressure (solid lines with closed circles and diamonds, respectively) and the rate of change with pressure (dashed lines with open circles and diamonds, respectively) derived from the fits to the RXES spectra. The values are underestimated. See text.

spectrum is scaled to the $h\nu_{in}$ axis in the PFY-XAS spectrum in Fig. 1(a). Spectral features strongly depend on $h\nu_{in}$ and the intensity of the spectra increases together with the PFY-XAS intensity as a function of $h\nu_{in}$. The spectrum measured at $h\nu_{in} = 8920$ eV, far below the Yb L_3 edge, already begins to exhibit two structures at $\Delta h\nu = 1522$ and 1530 eV. The structure at $\Delta h\nu = 1522$ eV is gradually enhanced with increasing $h\nu_{in}$ staying at $\Delta h\nu = 1522$ eV, and the intensity becomes maximum around $h\nu = 8938$ eV, corresponding to the Yb^{2+} absorption peak in the PFY-XAS spectrum. This indicates the structure at $\Delta h\nu = 1522$ eV is due to the Raman feature ascribed to the Yb^{2+} state. Consequently, the weaker structure at $\Delta h\nu = 1530$ eV is attributed to the Yb^{3+}-derived Raman feature. A prominent peak with a shift toward the higher $\Delta h\nu$ side with increasing $h\nu_{in}$ observed at high $h\nu_{in}$ is the $L\alpha_1$ fluorescence line peaked at $h\nu_{out} = 7416$ eV. The Raman features are still weakly detected at high $h\nu_{in}$ above the Yb^{3+} absorption peak. The $h\nu_{in}$ dependence of the RXES spectra are presented as a two-dimensional image plot in Fig. 1(c).

The RXES spectra in Fig. 1(b) are fitted with the Yb^{2+}- and Yb^{3+}-derived Raman components and the fluorescence component, assuming Voigt functions. The intensities are plotted as a function of $h\nu_{in}$ in Fig. 1(d) together with the PFY-XAS spectrum. Our result clearly shows the two Raman components originated from the Yb^{2+} and Yb^{3+} states. The Yb^{2+} and Yb^{3+} Raman peaks are enhanced at the corresponding peaks in the PFY-XAS spectrum. The ratio of the area intensity of the Yb^{2+} and Yb^{3+} Raman components shows the Yb valence to be $v = 2.51 \pm 0.05$, roughly consistent with the results derived from the fits to the PFY-XAS spectra [Fig. 2(c)].

B. Pressure dependence

Figure 2(a) shows the pressure dependence of PFY-XAS spectra of $YbNiGe_3$ at 300 K. A drastic change with pressure was observed. The intensities of the Yb^{2+} peak at $h\nu_{in} = 8938$ eV and Yb^{3+} peak at $h\nu_{in} = 8945$ eV are comparable. The spectral weight is continuously transferred from the Yb^{2+} to Yb^{3+} peaks with pressure, indicating that the Yb ion approaches the trivalent state as observed in many other Yb compounds [9–11,16,17,23]. We carried out the analyses by fits to the PFY-XAS spectra in Fig. 2(a) in order to quantitatively derive the Yb valence. An example of the fit to the spectrum at 15.6 GPa is shown in Fig. 2(b). We assumed the Gaussian functions for both the Yb^{2+} and Yb^{3+} components, and also for the QP component. Broad peaks due to the EXAFS were also approximated by the Gaussian functions. The relative intensity between Yb^{2+}- and Yb^{3+}-originated arctangent back grounds was fixed to that between the Yb^{2+} and Yb^{3+} Gaussian functions.

The Yb valences at 300 and 17 K are estimated as shown in Fig. 2(c) from the fits using an expression of $v = 2 + I_{3+}/(I_{2+} + I_{3+})$, where I_{2+} and I_{3+} are intensities of the Yb^{2+} and Yb^{3+} components, respectively. The Yb valence at 300 K is evaluated to be $v = 2.52 \pm 0.01$ at ambient pressure, indicating that the Yb valence in $YbNiGe_3$ strongly fluctuates and the Yb^{2+} and Yb^{3+} ions are almost equally distributed in the compound. The Yb valence increases rapidly with pressure to ~5 GPa, gradually to ~10 GPa, and reaches $v \sim 2.87$ at 15.6 GPa. The slope of the $v(P)$ curve changes between 5 and 10 GPa. Note that the QCP in $YbNiGe_3$ was suggested to be located at ~8 GPa from resistivity measurements [14]. Pressure derivatives of the Yb valence (dv/dP) are plotted by a red dashed line with open circles in the figure. The value of dv/dP drops between 5 and 10 GPa apart from 2.7 GPa. Above 8 GPa, it slowly decreases to nearly zero at 15.6 GPa. This behavior suggests that the Yb valence nearly saturates above 15.6 GPa and the Yb valence in $YbNiGe_3$ keeps fluctuating far below $v = 3$ even at high pressures.

The Yb valence at 17 K is slightly smaller compared to that at 300 K and monotonously increases with pressure as in the case at 300 K; $v \sim 2.45$ at ambient pressure and $v \sim 2.72$ at 7.7 GPa. The slope of the $v(P)$ curve at 17 K is also slightly smaller. The difference of the valences between 300 and 17 K becomes large at high pressures. This can qualitatively be understood as a result of the decrease of the Kondo temperature T_K with pressure as discussed later.

The pressure dependence of the Yb valence, in particular, between 5 and 10 GPa at 300 K, is also confirmed from the RXES spectra. Figure 2(d) shows the RXES spectra of $YbNiGe_3$ at 300 K measured under the same experimental conditions as in the PFY-XAS spectra in Fig. 2(a). The excitation energy is selected to be $h\nu_{in} = 8934$ eV, 4 eV below the Yb^{2+} absorption peak, in order to detect the Yb^{2+} and Yb^{3+} components with relatively equal weight [Fig. 1(d)]. A shoulder structure at $\Delta h\nu = 1520$ eV, which is most prominent in the spectrum at 15.6 GPa, is attributed to the fluorescence line with $h\nu_{out} = 7416$ eV. The QP structure, which should be accompanied by the Yb^{2+} peak, is not observed here, probably due to its negligibly small contribution to the RXES spectra. An example of the fit to the RXES spectrum at 15.6 GPa is shown in Fig. 2(e). We assume Gaussian functions for the Yb^{2+} and fluorescence structures, while two functions, the Gaussian function and the Voigt function taking into account an antisymmetry, are required to fit the Yb^{3+}-derived structure because it has a long tail to the higher $\Delta h\nu$ side. From the fits, we tentatively estimated the Yb valence using the same formula described above, as shown in Fig. 2(f). The trend of the pressure- and temperature-dependent Yb valence is, thus, in overall agreement with that observed in the PFY-XAS measurements [Fig. 2(c)], apart from the absolute value. The Yb valences derived from the RXES measurements in Fig. 2(f) are lower than those from the PFY-XAS measurements in Fig. 2(c). Note that the intensity ratio between the Yb^{2+} and Yb^{3+} components in the RXES spectra does not provide an absolute value of the valence due to the resonance effect. As noticed from Fig. 1(d), the intensity ratio strongly depends on $h\nu_{in}$; the Yb^{2+} and Yb^{3+} components are most enhanced at the corresponding peak in the PFY-XAS spectra. The excitation energy of $h\nu_{in} = 8934$ eV is close to the Yb^{2+} absorption peak and the Yb^{2+} contribution to the RXES spectra is somewhat larger than the Yb^{3+} contribution, which results in a low value of the Yb valence. Therefore, the PFY-XAS analyses give the reliable results of the absolute Yb valence [Fig. 2(c)].

The increase of the Yb^{3+} component with pressure should be reflected to the QP component in the PFY-XAS spectra, because the empty $4f$ state comes only from the Yb^{3+} ion. In fact, we were able to resolve an enhancement of the QP component with pressure by careful fits to the PFY-XAS

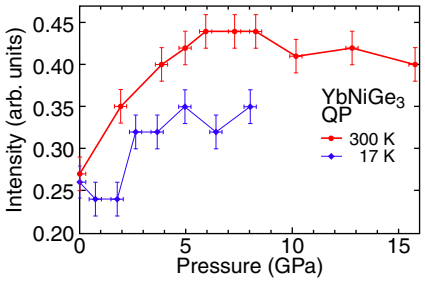

FIG. 3. (Color online) Intensities of the quadrupole component as a function of pressure.

spectra as shown in Fig. 3. We find roughly the same trend for the pressure-induced change in the QP intensity as that in the Yb valence in Figs. 2(c) and 2(f). In other words, the result in Fig. 3 supports the assignment of the weak shoulder below the Yb^{2+} absorption peak in the PFY-XAS spectra to the QP transition [24].

C. Temperature dependence

The results of the temperature-dependent PFY-XAS and RXES experiments for $YbNiGe_3$ and $YbNiSi_3$ are summarized in Fig. 4. In contrast to the PFY-XAS spectra of $YbNiGe_3$ in Fig. 4(a), almost only the Yb^{3+} peak is observed in those of $YbNiSi_3$ in Fig. 4(c). The Yb^{3+} peak has a long tail toward the higher $h\nu_{in}$ side. This long tail has been observed in the PFY-XAS spectra of $YbNi_3Al_9$, where the Yb valence is also very close to 3 [25] as is the case for $YbNiSi_3$. A small peak at $h\nu_{in} = 8934$ eV is attributed to the QP transition. The Yb^{2+} contribution is weakly observed as a structure slightly filling between the QP and Yb^{3+} structures, indicating a small fraction of the Yb $^{2+}$ ion. An existence of the Yb^{2+} ion in $YbNiSi_3$ is further clearly evidenced in the RXES spectra in Fig. 4(d). Since the RXES spectra are taken at the Yb^{2+} absorption peak ($h\nu_{in} = 8938$ eV), the intensity of the Yb^{2+} peak is resonantly enhanced at $\Delta h\nu = 1523$ eV.

The temperature dependencies of the Yb valences in $YbNiGe_3$ and $YbNiSi_3$ are shown in Fig. 4(e) derived from the analyses by fits to the PFY-XAS spectra. The Gaussian function and Voigt function taking into account an antisymmetry are required to fit the long tail of the Yb^{3+} structure of $YbNiSi_3$. The Yb valence in $YbNiGe_3$ slightly decreases down to 100 K and does not demonstrably change below 100 K. The estimated valences are $v \sim 2.55$ at 299 K and $v \sim 2.48$ at 8 K. Such decrease of the valence has been observed in many other Yb-based valence fluctuating compounds [16,23,25,26]. According to the single impurity Anderson model with noncrossing approximation, the Yb valence rapidly decreases at $T < T_K$ and takes a constant value at sufficiently low temperature [27]. The almost unchanged Yb valence below 100 K suggests a high T_K for $YbNiGe_3$, as inferred from the magnetic susceptibility with a maximal temperature of ~300 K [12].

The Yb valence in $YbNiSi_3$ is close to 3 with almost no temperature dependence from the fits to the PFY-XAS spectra. On the other hand, the Yb^{2+} peak in the RXES spectra in Fig. 4(d) seems to be slightly reduced with decreasing temperature. Figure 4(f) shows the Yb valence derived from the fits to the RXES spectra. Note that the Yb valence in Fig. 4(f) is underestimated since the Yb^{2+} contribution is noticeable in the RXES spectra measured at the Yb^{2+} absorption peak. One notices that overall the Yb valence slightly decreases with lowering temperature. The result in Fig. 4(f) suggests that the Yb ion tends to favor the Yb^{2+} state with temperature even for the compounds with the Yb valence close to 3.

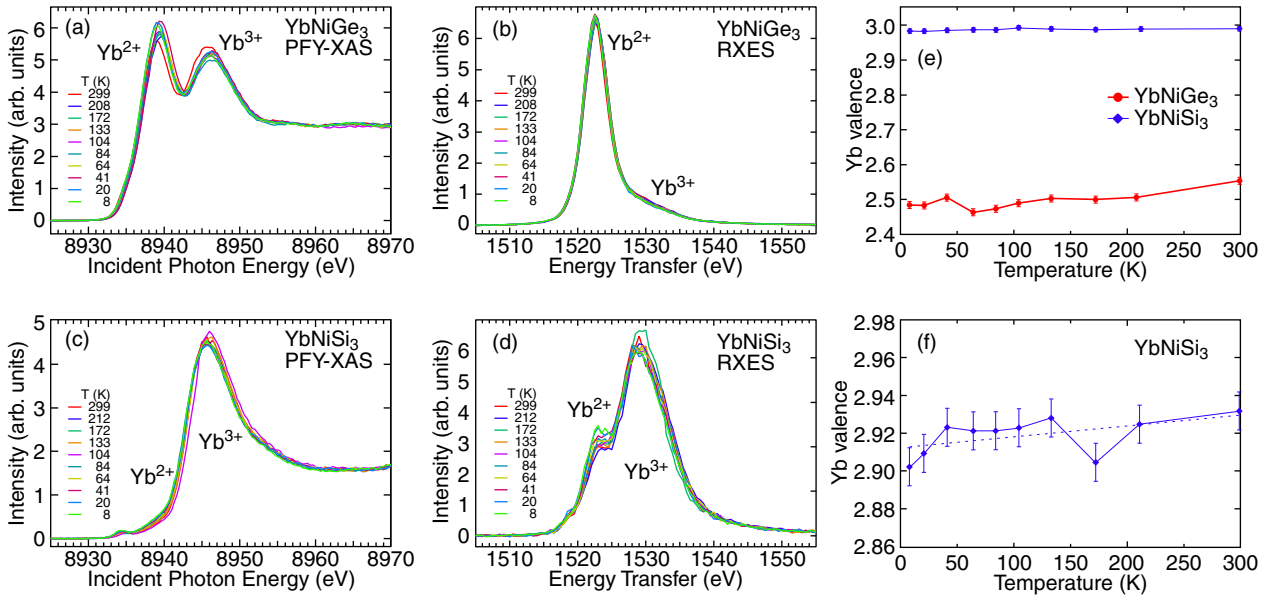

FIG. 4. (Color online) Temperature dependencies of the PFY-XAS spectra of $YbNiGe_3$ (a) and $YbNiSi_3$ (b) around the Yb L_3 absorption edge measured at ambient pressure, and those of RXES spectra of $YbNiGe_3$ (c) and $YbNiSi_3$ (d) excited with $h\nu_{in} = 8938$ eV. (e) Temperature dependencies of the Yb valences in $YbNiGe_3$ and $YbNiSi_3$ derived from the fits to the PFY-XAS spectra. (f) Temperature dependence of the Yb valence in $YbNiSi_3$ derived from the fits to the RXES spectra. The values are underestimated. The dashed line is a linear fit to the valence.

IV. DISCUSSION

The most important finding in the present study is that the slope of the $v(P)$ curve at 300 K gets lower between 5 and 10 GPa. This result on $YbNiGe_3$ is reminiscent of that on $YbCu_2Si_2$ [9]. Fernandez-Pañella *et al.* investigated the Yb valence in $YbCu_2Si_2$ under pressures up to 22 GPa by means of PFY-XAS and Yb RXES around the Yb L_3 absorption edge. Note that in this case $YbCu_2Si_2$ exhibits a pressure-induced ferromagnetic order at the critical pressure of $P_c \sim 8$ GPa [8]. The Yb valence of $v \sim 2.84$ at ambient pressure increases toward Yb^{3+} with pressure at 300 K. The pressure effect on the valence becomes weak at 9–11 GPa, comparable to P_c, and the valence gradually reaches $v \sim 2.95$ at 22 GPa. They carried out the experiments at 7, 15, and 300 K, which are all higher than the ferromagnetic order temperature ($T_C \sim 6$ K), and found that the slope change was still observed at 300 K, far above T_C. A similar slope change in the $v(P)$ curve at 300 K was also reported for YbCuAl [11] with the pressure-induced magnetic ordering around 8 GPa [28] and $YbNi_2Ge_2$ [10] with ordering around 5 GPa [29].

As mentioned previously, Umeo *et al.* [14] reported the electrical resistivity of the single-crystalline $YbNiGe_3$ under pressures up to 6.5 GPa and at temperatures down to 0.3 K. The maximal temperature T_{max} in the magnetic contribution to the resistivity decreased linearly with pressure, reflecting the lowering of T_K by pressurization since T_{max} usually scales with T_K [30]. The authors analyzed $\rho(T)$ in the low temperature region with the form of $\rho(T) = \rho_0 + AT^n$. The A coefficient increases by a factor of 10 with pressure from 3.6 to 6.5 GPa and ρ_0 is also enhanced steeply above 4.8 GPa. From these results, it is suggested that the ground state of $YbNiGe_3$ at 6.5 GPa is close to the QCP, which should be at approximately 8 GPa. The slop change in the $v(P)$ curve observed for $YbNiGe_3$ is considered to be strongly correlated to the pressure dependence of the resistivity [14]. The concomitant enhancements of both A and ρ_0 with increasing pressure toward P_c were also observed in $YbCu_2Si_2$ and the existence of the QCP is evidenced by the magnetic susceptibility and specific heat measurements [8,31]. The magnetic order has not directly been found above 6.5 GPa in $YbNiGe_3$ at present. In order to examine the existence of such magnetic ordering, further magnetic susceptibility and specific heat measurements under higher pressures are planned.

The Yb valences at ambient pressure are $v \sim 2.84$ for $YbCu_2Si_2$ [9], $v \sim 2.93$ for $YbNi_2Ge_2$ [10], and $v \sim 2.93$ for YbCuAl [11] at 300 K. The Yb valences become close to the trivalent state at high pressures, $v \sim 2.98$ (22.0 GPa) for $YbCu_2Si_2$, $v \sim 2.98$ (25.2 GPa) for $YbNi_2Ge_2$, and $v \sim 2.97$ (16.5 GPa) for YbCuAl. Compared to these compounds, the Yb valence in $YbNiGe_3$ more strongly fluctuates still at high pressures [Fig. 2(c)]. In particular, the valence seems to almost saturate with $v \sim 2.87$, far below the fully trivalent state. Note that the Yb valence in $YbNiSi_3$ with antiferromagnetic ordering below $T_N = 5.1$ K is $v \sim 3$ even at room temperature [Fig. 4(e)], though it is expected that the electronic state of $YbNiGe_3$ should approach that of $YbNiSi_3$ with pressure due to the lattice contraction. The low valence state of $YbNiGe_3$ at high pressures indicates that the hybridization strength between the Yb $4f$ and conduction-band electrons is still present under high pressure.

A similar result is observed for a valence fluctuating compound $YbNi_3Ga_9$, which was recently discovered together with an antiferromagnet $YbNi_3Al_9$ [32,33]. In $YbNi_3Ga_9$, the magnetic ordering occurs at $P_c \sim 9$ GPa [34]. Pressure-dependent XAS studies revealed that the Yb valence is $v \sim 2.69$ at ambient pressure and fluctuates even above P_c with $v \sim 2.89$ (16 GPa) at 300 K [35]. Our experimental results on $YbNiGe_3$ together with those on $YbNi_3Ga_9$ suggest that, well before Yb reaches the fully trivalent state, Yb begins to behave as a magnetic ion and intersite magnetic fluctuations begin to be enhanced in strong valence fluctuating compounds.

From Fig. 2(c) we notice that the Yb valence in $YbNiGe_3$ rapidly increases with pressure up to 5 GPa. Such a large pressure dependence is qualitatively understood from the shift of the Yb^{2+} $4f_{7/2}$ level relative to E_F. In the hard x-ray photoemission spectra in the valence bands of $YbNiGe_3$, the Yb^{2+} $4f_{7/2}$ level is centered at 0.15 eV below E_F, and has some weight at E_F [36]. The Yb^{2+} $4f$ level goes toward the E_F side with pressure and the $4f$ electron is easily transferred into the lowest unoccupied conduction-band density of states (DOS) such as Yb $5d$. The saturation of the Yb valence at high pressures suggests that the low DOS region (pseudo-gap-like region) exists slightly above the Fermi level (E_F). Further studies on $YbNiGe_3$ are required with respect to the origin of the low valence at high pressures, including band-structure calculations.

The large pressure dependence of the Yb valence is also consistent with the pressure dependence of the magnetic susceptibilities. Zell *et al.* [37] pointed out that the susceptibility is most sensitive to pressure when the Yb valence is $v = 2.5$ at ambient pressure, namely equal population of the Yb^{2+} and Yb^{3+} states, which is the just case for $YbNiGe_3$ by the present PFY-XAS experiments.

In the present experiments on $YbNiGe_3$ at 17 K, we applied the pressure only up to 7.7 GPa, which is slightly lower than pressure where the slope change is observed at 300 K, because of a technical limitation. In comparison with the results of $YbCu_2Si_2$ [9], we believe that the slope change should be observed above 8 GPa also at 17 K [38].

In the recent studies on the temperature dependence of the Yb valence in $YbNi_3Ga_9$ at ambient pressure by means of the PFY-XAS [25], the valences were estimated to be $v \sim 2.68$ at 300 K and $v \sim 2.53$ at 23 K, slightly close to Yb^{3+} compared to $YbNiGe_3$. The valence monotonically decreases down to 23 K and its decrease rate with temperature is larger compared to that for $YbNiGe_3$. Since T_K of $YbNi_3Ga_9$ was estimated to be 570 K from the magnetic susceptibility measurements [33], the weak temperature dependence of the valence for $YbNiGe_3$ suggests higher T_K than for $YbNi_3Ga_9$. This result is qualitatively consistent with the magnetic susceptibility; it has a broad maximum around 200 K for $YbNi_3Ga_9$ [33], while around 300 K for $YbNiGe_3$ [12], which is a signature of the higher T_K for $YbNiGe_3$.

The same argument would be valid for the pressure dependence of the Yb valence in $YbNiGe_3$ measured at 300 and 17 K. From Fig. 2(c) the slope of the $v(P)$ curve at 17 K is slightly gradual compared to that at 300 K. The decrement of the valence between 17 and 300 K increases with pressure. These results mean that the decrease rate with temperature is more pronounced at higher pressure and are understood

qualitatively as a result of the lowering of T_K by pressurization, which is indicated by the decrease of T_{max} in the electrical resistivity [14].

V. CONCLUSION

We have investigated the Yb valence in $YbNiGe_3$ under pressures up to 15.6 GPa at 300 K and up to 7.7 GPa at 17 K by means of PFY-XAS and RXES around the Yb L_3 absorption edge. The strong pressure dependence of the Yb valence toward Yb^{3+} is observed at 300 K. The valence of $v \sim 2.52$ rapidly increases with pressure to ~5 GPa and reaches a saturated value of $v \sim 2.87$ at 15.6 GPa. A change in the slope of the $v(P)$ curve is detected between 5 and 10 GPa, where the steep enhancements of both A and ρ_0 were observed and the existence of the QCP was suggested [14]. The slope change is closely related to the transition of the magnetic ordered phase, in comparison with the results of $YbCu_2Si_2$ [9], $YbNi_2Ge_2$ [10], and YbCuAl [11] with pressure-induced magnetic orderings. In contrast to these compounds with nearly Yb^{3+} state, the valence in $YbNiGe_3$ still fluctuates at high pressures, indicating that the hybridization between the $4f$ and conduction electrons remains present. This result suggests that, well before Yb reaches the fully trivalent state, Yb begins to behave as a magnetic ion and the intersite magnetic fluctuations begin to be enhanced in the strong valence fluctuating compounds. The Yb valence in $YbNiGe_3$ decreases to $v \sim 2.45$ at ambient pressure at 17 K. Although the valence increases with pressure at 17 K, the increment is relatively small compared to that at 300 K. This is qualitatively understood as a result of the decrease of T_K with pressure. The QP intensity changes with the same manner as the Yb valence under pressure, indicating that it indeed reflects the empty $4f$ state. We also investigated the temperature dependence of the Yb valences in $YbNiSi_3$ for comparison. In spite of their similar crystal structure and conduction electronic states, the Yb valence in $YbNiSi_3$ is close to 3 and shows little temperature dependence. The Yb valence in $YbNiGe_3$ decreases with lowering temperature as the other valence fluctuating compounds. The decreasing rate with lowering temperature is relatively small, which reflects its high T_K.

ACKNOWLEDGMENTS

The authors are grateful to K. Ohta and J. Kodama for their support during the experiments. They also thank Professor S. Ohara for valuable comments for the Yb valence at high pressure and Professor J. Ghijsen for critical reading of our manuscript. The experiments at SPring-8 were performed under the approval of Taiwan Beamline (SPring-8 Proposal No. 2012B425, NSRRC Proposal No. 2012-1-017). This work was partly supported by Grant in Aid for Scientific Researches (Grants No. 22540343, No. 22340103, and No. 23540411) from the Japan Society for the Promotion of Science in Japan. The work at UT Austin was supported as part of EFree, an Energy Frontier Research Center funded by the US Department of Energy Office of Science, Office of Basic Energy Sciences under Award DE-SC0001057. M.A.A. and R.A.R. acknowledge the financial support of FAPESP (Grants No. 2011/19924-2, No. 2011/23795-3, and No. 2012/17562-9).

[1] S. Doniach, Physica B & C **91**, 231 (1977).
[2] R. Settai, T. Takeuchi, and Y. Ōnuki, J. Phys. Soc. Jpn. **76**, 051003 (2007).
[3] P. Monthoux, D. Pines, and G. G. Lonzarich, Nature (London) **450**, 1177 (2007).
[4] P. Gegenwart, Q. Si, and F. Steglich, Nat. Phys. **4**, 186 (2008).
[5] S. Nakatsuji, K. Kuga, Y. Machida, T. Tayama, T. Sakakibara, Y. Karaki, H. Ishimoto, S. Yonezawa, Y. Maeno, E. Pearson, G. G. Lonzarich, L. Balicas, H. Lee, and Z. Fisk, Nat. Phys. **4**, 603 (2008).
[6] M. Okawa, M. Matsunami, K. Ishizaka, R. Eguchi, M. Taguchi, A. Chainani, Y. Takata, M. Yabashi, K. Tamasaku, Y. Nishino, T. Ishikawa, K. Kuga, N. Horie, S. Nakatsuji, and S. Shin, Phys. Rev. Lett. **104**, 247201 (2010).
[7] S. Watanabe and K. Miyake, Phys. Rev. Lett. **105**, 186403 (2010).
[8] A. Fernandez-Pañella, D. Braithwaite, B. Salce, G. Lapertot, and J. Flouquet, Phys. Rev. B **84**, 134416 (2011).
[9] A. Fernandez-Pañella, V. Balédent, D. Braithwaite, L. Paolasini, R. Verbeni, G. Lapertot, and J.-P. Rueff, Phys. Rev. B **86**, 125104 (2012).
[10] H. Yamaoka, I. Jarrige, N. Tsujii, J.-F. Lin, N. Hiraoka, H. Ishii, and K.-D. Tsuei, Phys. Rev. B **82**, 035111 (2010).
[11] H. Yamaoka, N. Tsujii, Y. Utsumi, H. Sato, I. Jarrige, Y. Yamamoto, J.-F. Lin, N. Hiraoka, H. Ishii, K.-D. Tsuei, and J. Mizuki, Phys. Rev. B **87**, 205120 (2013).
[12] E. D. Mun, S. L. Bud'ko, H. Ko, G. J. Miller, and P. C. Canfield, J. Magn. Magn. Mater. **322**, 3257 (2010).
[13] M. A. Avila, M. Sera, and T. Takabatake, Phys. Rev. B **70**, 100409 (2004).
[14] K. Umeo, N. Hosogi, M. A. Avila, and T. Takabatake, Phys. Status Solidi B **247**, 751 (2010).
[15] T. Moriya and T. Takimoto, J. Phys. Soc. Jpn. **64**, 960 (1995).
[16] H. Yamaoka, I. Jarrige, N. Tsujii, N. Hiraoka, H. Ishii, and K.-D. Tsuei, Phys. Rev. B **80**, 035120 (2009).
[17] H. Yamaoka, I. Jarrige, N. Tsujii, M. Imai, J.-F. Lin, M. Matsunami, R. Eguchi, M. Arita, K. Shimada, H. Namatame, M. Taniguchi, M. Taguchi, Y. Senba, H. Ohashi, N. Hiraoka, H. Ishii, and K.-D. Tsuei, Phys. Rev. B **83**, 104525 (2011).
[18] H. Yamaoka, I. Jarrige, N. Tsujii, J.-F. Lin, T. Ikeno, Y. Isikawa, K. Nishimura, R. Higashinaka, H. Sato, N. Hiraoka, H. Ishii, and K.-D. Tsuei, Phys. Rev. Lett. **107**, 177203 (2011).
[19] J.-P. Rueff and A. Shukla, Rev. Mod. Phys. **82**, 847 (2010).
[20] Y. Feng, R. Jaramillo, J. Wang, Y. Ren, and T. F. Rosenbaum, Rev. Sci. Instrum. **81**, 041301 (2010).
[21] H. Yamaoka, Y. Zekko, I. Jarrige, J.-F. Lin, N. Hiraoka, H. Ishii, K.-D. Tsuei, and J. Mizuki, J. Appl. Phys. **112**, 124503 (2012).
[22] C.-S. Zha, H.-K. Mao, and R. J. Hemley, Proc. Natl. Acad. Sci. USA **97**, 13494 (2000).
[23] L. Moreschini, C. Dallera, J. J. Joyce, J. L. Sarrao, E. D. Bauer, V. Fritsch, S. Bobev, E. Carpene, S. Huotari,

G. Vankó, G. Monaco, P. Lacovig, G. Panaccione, A. Fondacaro, G. Paolicelli, P. Torelli, and M. Grioni, Phys. Rev. B **75**, 035113 (2007).

[24] Although the analyzed QP intensity seems saturate still above ∼5 Pa and to slightly decrease at high temperatures, we consider here that its trend is almost the same as that of the Yb valence within the present analytical accuracy, because the QP structure is only observed as the weak shoulder of the Yb^{2+} peak.

[25] Y. Utsumi, H. Sato, S. Ohara, T. Yamashita, K. Mimura, S. Motonami, K. Shimada, S. Ueda, K. Kobayashi, H. Yamaoka, N. Tsujii, N. Hiraoka, H. Namatame, and M. Taniguchi, Phys. Rev. B **86**, 115114 (2012).

[26] J. Yamaguchi, A. Sekiyama, S. Imada, H. Fujiwara, M. Yano, T. Miyamachi, G. Funabashi, M. Obara, A. Higashiya, K. Tamasaku, M. Yabashi, T. Ishikawa, F. Iga, T. Takabatake, and S. Suga, Phys. Rev. B **79**, 125121 (2009).

[27] L. H. Tjeng, S.-J. Oh, E.-J. Cho, H.-J. Lin, C. T. Chen, G.-H. Gweon, J.-H. Park, J. W. Allen, T. Suzuki, M. S. Makivić, and D. L. Cox, Phys. Rev. Lett. **71**, 1419 (1993).

[28] K. Alami-Yadri, H. Wilhelm, and D. Jaccard, Solid State Commun. **108**, 279 (1998).

[29] G. Knebel, D. Braithwaite, G. Lapertot, P. C. Canfield, and J. Flouquet, J. Phys.: Condens. Matter **13**, 10935 (2001).

[30] H. Q. Yuan, M. Nicklas, Z. Hossain, C. Geibel, and F. Steglich, Phys. Rev. B **74**, 212403 (2006).

[31] E. Colombier, D. Braithwaite, G. Lapertot, B. Salce, and G. Knebel, Phys. Rev. B **79**, 245113 (2009).

[32] S. Ohara, T. Yamashita, Y. Mori, and I. Sakamoto, J. Phys.: Conf. Ser. **273**, 012048 (2011).

[33] T. Yamashita, R. Miyazaki, Y. Aoki, and S. Ohara, J. Phys. Soc. Jpn. **81**, 034705 (2012).

[34] S. Ohara (private communication).

[35] K. Matsubayashi (private communication).

[36] H. Sato *et al*. (unpublished).

[37] W. Zell, R. Pott, B. Roden, and D. Wohlleben, Solid State Commun. J. Phys. Soc. Jpn. **40**, 751 (1981).

[38] The slope change in the $v(P)$ curve at 7 K is not so remarkable compared to that at 300 K in case of $YbCu_2Si_2$ [9].